

Robust Control and \mathcal{H}_∞ -Optimization—Tutorial Paper*

HUIBERT KWAKERNAAK†

Robust control systems may successfully be designed by \mathcal{H}_∞ -optimization, in particular, by reformulating the design problem as a mixed sensitivity problem.

Key Words— \mathcal{H}_∞ -optimal control; robust control.

Abstract—The paper presents a tutorial exposition of \mathcal{H}_∞ -optimal regulation theory, emphasizing the relevance of the mixed sensitivity problem for robust control system design.

1. INTRODUCTION

THE INVESTIGATION OF \mathcal{H}_∞ -optimization of control systems began in 1979 with a conference paper by Zames (1979), who considered the minimization of the ∞ -norm of the sensitivity function of a single-input–single-output linear feedback system. The work dealt with some of the basic questions of “classical” control theory, and immediately caught a great deal of attention. It was soon extended to more general problems, in particular when it was recognized that the approach allows dealing with robustness far more directly than other optimization methods.

The name “ \mathcal{H}_∞ -optimization” is somewhat unfortunate. \mathcal{H}_∞ is one member of the family of spaces introduced by the mathematician Hardy. It is the space of functions on the complex plane that are analytic and bounded in the right-half plane. The space plays an important role in the deeper mathematics needed to solve \mathcal{H}_∞ -optimal control problems.

This paper presents a tutorial exposition of the subject. The emphasis is on explaining the relevance of \mathcal{H}_∞ -optimization for control engineering. The paper presents few new results, and does not at all do justice to the extensive theoretical and mathematical literature on the subject. The presentation is limited to single-input–single-output (SISO) control systems. Many of the arguments carry over to the multi-input–

multi-output case but their implementation is necessarily more complex.

We preview some of the contents. In Section 2 we use Zames’ original minimum-sensitivity problem to introduce \mathcal{H}_∞ -optimization. Section 3 is devoted to a discussion of stability robustness. A well-known stability robustness criterion first proposed by Doyle (1979) demonstrates the relevance of the ∞ -norm for robustness. Doyle’s criterion in its original form has severe shortcomings, owing to the oversimplified representation of plant perturbations. In Section 4 it is explained how the criterion quite easily can be extended to a much more powerful result that applies to a very general perturbation model. In Section 5 this result is used for a perturbation model that for lack of a better name we refer to as numerator–denominator perturbations. It leads to the “mixed sensitivity” \mathcal{H}_∞ stability robustness test. It is only slightly more complicated than Doyle’s original test, and far less conservative for low-frequency perturbations.

Minimization of the mixed sensitivity criterion results in “optimal” robustness. In Section 6 the resulting mixed sensitivity problem is discussed in some detail. It is shown that it can be used not only for robustness optimization or robustness improvement, but also for design for performance. The design method based on the mixed sensitivity criterion features frequency response shaping, type k control and specified high-frequency roll-off, and direct control over the closed-loop bandwidth and time response by means of dominant pole placement.

To illustrate these features two design examples are included. In Section 7 a textbook example is discussed that is simple enough to be completely transparent. In Section 8 the application of the mixed sensitivity method to a benchmark example involving ship course control is described.

Sections 9–11 briefly review the theory needed to solve \mathcal{H}_∞ -optimal regulation problems. In Section 9 it is shown that the mixed sensitivity problem is a special case of the so-called “standard” \mathcal{H}_∞ -optimal regulation problem. In Section 10 the frequency domain solution of the standard problem is outlined, while Section 11 describes the main features of the state space solution.

* Received 6 February 1992; revised 6 July 1992; received in final form 23 August 1992. The original version of this paper was presented at the IFAC Symposium on Design Methods of Control Systems which was held in Zürich, Switzerland during September 1991. The Published Proceedings of this IFAC Meeting may be ordered from: Pergamon Press Ltd, Headington Hill Hall, Oxford, OX3 0BW, U.K. This paper was recommended for publication in revised form by Editor K. J. Åström.

† Systems and Control Group, Department of Applied Mathematics, University of Twente, P.O. Box 217, 7500 AE Enschede, The Netherlands.

We do not go into much detail, because the theory is not easy, and the development of algorithms that can be used unthinkingly for applications is best left to specialists.

2. SENSITIVITY

\mathcal{H}_∞ -optimization of control systems deals with the minimization of the peak value of certain closed-loop frequency response functions. To clarify this, consider by way of example the basic SISO feedback system of Fig. 1. The plant has transfer function P and the compensator has transfer function C . The signal v represents a disturbance acting on the system and z is the control system output. Then from the signal balance equation $\hat{z} = \hat{v} - PC\hat{z}$, with the circumflex denoting the Laplace transform, it follows that $\hat{z} = S\hat{v}$, where

$$S = \frac{1}{1 + PC}, \tag{1}$$

is the sensitivity function of the feedback system. As the name implies, the sensitivity function characterizes the sensitivity of the control system output to disturbances. Ideally, $S = 0$.

The problem originally considered by Zames (1979, 1981) is that of finding a compensator C that makes the closed-loop system stable and minimizes the peak value of the sensitivity function. This peak value (see Fig. 2) is defined as

$$\|S\|_\infty = \max_{\omega \in \mathbb{R}} |S(j\omega)|, \tag{2}$$

where \mathbb{R} denotes the set of real numbers. Because for some functions the peak value may not be assumed for any finite frequency, we replace the maximum

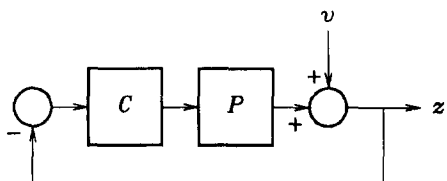


FIG. 1. SISO feedback loop.

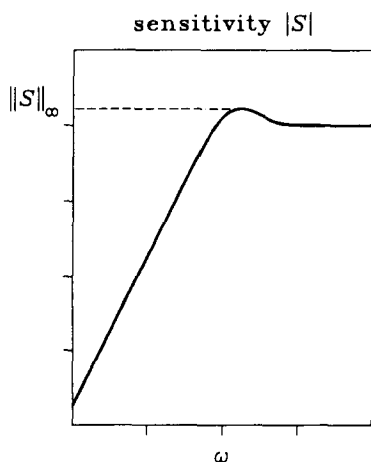


FIG. 2. $\|S\|_\infty$ as peak value.

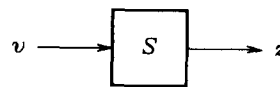


FIG. 3. Equivalent representation of the system of Fig. 1.

here and in the following by the supremum or least upper bound, so that

$$\|S\|_\infty = \sup_{\omega \in \mathbb{R}} |S(j\omega)|. \tag{3}$$

The justification of this problem is that if the peak value $\|S\|_\infty$ of the sensitivity function S is small, then the magnitude of S necessarily is small for all frequencies, so that disturbances are uniformly attenuated over all frequencies. Minimization of $\|S\|_\infty$ is worst-case optimization, because it amounts to minimizing the effect on the output of the worst disturbance (namely, a harmonic disturbance at the frequency where $|S|$ has its peak value).

The worst-case model has an important mathematical interpretation. Suppose that the disturbance v has unknown frequency content, but finite energy $\|v\|_2^2$. The number

$$\|v\|_2 = \sqrt{\int_{-\infty}^{\infty} |v(t)|^2 dt}, \tag{4}$$

is known as the 2-norm of the disturbance v . The energy of v is the square of the 2-norm. Then the norm $\|S\|$ of the system S as in Fig. 3 with input v and output z induced by the 2-norm is defined as

$$\|S\| = \sup_{v: \|v\|_2 < \infty} \frac{\|z\|_2}{\|v\|_2}. \tag{5}$$

Hence, in engineering terms the norm is directly related to the energy gain for the input with the worst possible frequency distribution. Using Parseval's theorem, it is not difficult to recognize that

$$\|S\| = \|S\|_\infty. \tag{6}$$

Hence, the peak value is precisely the norm of the system induced by the 2-norms on the input and output signals. This norm is known as the ∞ -norm of the system.

It follows that \mathcal{H}_∞ -optimization is concerned with the minimization of system norms. It is useful to be aware of this when studying theoretical papers on \mathcal{H}_∞ -optimization.

Worst-case optimization suggests a game theory paradigm: The designer wishes to determine the compensator C that offers the best protection against the worst disturbance that nature has in store. This explains why in many theoretical papers \mathcal{H}_∞ -optimization is treated from the point of view of differential game theory.

A little contemplation reveals that minimization of $\|S\|_\infty$ as it stands is not a useful design tool. The frequency response function of every physical plant and compensator decreases at high frequencies. This means that often the sensitivity S can be made small at low frequencies but eventually reaches the asymptotic value one for high frequencies. Just how small S is at low frequencies is not reflected in the peak value but is of paramount importance for the control system

performance. For this reason, it is customary to introduce a frequency dependent weighting function W and consider the minimization of

$$\|WS\|_\infty = \sup_{\omega \in \mathbb{R}} |W(j\omega S(j\omega))|. \quad (7)$$

Characteristically, W is large at low frequencies but decreases at high frequencies.

The weighted sensitivity minimization problem thus defined has interesting aspects. Unfortunately, it does not account adequately for basic bandwidth limitations owing to restricted plant capacity, caused by the inability of the plant to absorb inputs that are too large. Before going into this deeper we consider the question of robustness.

3. ROBUSTNESS

We illustrate the connection between peak value minimization and design for robustness by considering in Fig. 4 the Nyquist plot of the loop gain $L = PC$ of the SISO feedback system of Fig. 1. In particular, we study whether the feedback system remains stable under a perturbation of the loop gain from its nominal value L_0 to the actual value L .

For simplicity we take the system to be open-loop stable (that is, L represents a stable system). Naturally, we also assume that the nominal closed-loop system is well-designed so that it is stable. Then by the Nyquist stability criterion the Nyquist plot of the nominal loop gain L_0 does not encircle the point -1 . The actual closed-loop system is stable if also the loop gain L does not encircle the point -1 .

It is easy to see by inspection of Fig. 4 that the Nyquist plot L definitely does not encircle the point -1 if for every frequency ω the distance $|L(j\omega) - L_0(j\omega)|$ between any point $L(j\omega)$ on the plot of L and the corresponding point $L_0(j\omega)$ on the plot of L_0 is less than the distance $|L_0(j\omega) + 1|$ between the point $L_0(j\omega)$ and the point -1 , that is, if

$$|L(j\omega) - L_0(j\omega)| < |L_0(j\omega) + 1| \quad \text{for all } \omega \in \mathbb{R}. \quad (8)$$

This is equivalent to

$$\frac{|L(j\omega) - L_0(j\omega)|}{|L_0(j\omega)|} \cdot \frac{|L_0(j\omega)|}{|L_0(j\omega) + 1|} < 1, \quad \text{for all } \omega \in \mathbb{R}. \quad (9)$$

Define the complementary sensitivity function T_0 of the nominal closed-loop system as

$$T_0 = 1 - S_0 = 1 - \frac{1}{1 + L_0} = \frac{L_0}{1 + L_0}, \quad (10)$$

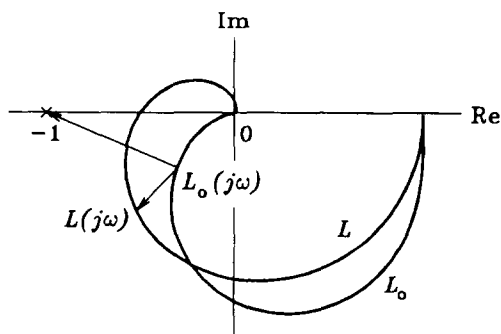


FIG. 4. Stability under perturbation.

with S_0 the nominal sensitivity function. Then it follows from (9) that if

$$\frac{|L(j\omega) - L_0(j\omega)|}{|L_0(j\omega)|} \cdot |T_0(j\omega)| < 1, \quad \text{for all } \omega \in \mathbb{R}, \quad (11)$$

the perturbed closed-loop system is stable.

The factor $|L(j\omega) - L_0(j\omega)|/|L_0(j\omega)|$ in this expression is the *relative* size of the perturbation of the loop gain L from its nominal value L_0 . Suppose that this relative perturbation as a function of frequency is known to be bounded by

$$\frac{|L(j\omega) - L_0(j\omega)|}{|L_0(j\omega)|} \leq |W(j\omega)|, \quad \text{for all } \omega \in \mathbb{R}, \quad (12)$$

with W a given frequency dependent function. Then

$$\begin{aligned} & \frac{|L(j\omega) - L_0(j\omega)|}{|L(j\omega)|} \cdot |T_0(j\omega)| \\ &= \frac{|L(j\omega) - L_0(j\omega)|/|L_0(j\omega)|}{|W(j\omega)|} \cdot |W(j\omega)T_0(j\omega)| \\ &< |W(j\omega)T_0(j\omega)|. \end{aligned} \quad (13)$$

Hence, if

$$|W(j\omega)T_0(j\omega)| < 1, \quad \text{for all } \omega \in \mathbb{R}, \quad (14)$$

by (11) the closed-loop system is stable for all perturbations bounded by (12). Indeed, it may be shown that the condition (14) is not only sufficient but also necessary for the closed-loop system to be stable for all perturbations bounded by (12).

We obtained the condition (14) under the assumption that the open-loop system is stable. It may be proved that it also holds for open-loop unstable systems, as long as the nominal and the perturbed open-loop system have the same number of right-half plane poles. The result may also be extended to multivariable systems (Doyle, 1979).

Using the norm notation introduced in (3) the condition (14) for robust stability may be rewritten as

$$\|WT_0\|_\infty < 1. \quad (15)$$

This explicitly demonstrates the relevance of the ∞ -norm, that is, the peak value, for robustness characterization. The peak value criterion arises from the Nyquist stability criterion, which forbids the Nyquist plot of the loop gain to cross the point -1 .

For stability robustness the feedback system need be designed such that $\|WT_0\|_\infty$ is less than one. It is tempting to consider the problem of minimizing the norm $\|WT_0\|_\infty$ with respect to all compensators that stabilize the closed-loop system as a way of optimizing robustness. Stability seldom is the sole design target, though, and robustness optimization may easily lead to useless results. If the system is open-loop stable, for instance, and all perturbations that may arise leave it stable, $\|WT_0\|_\infty$ may be made equal to zero, and hence, minimal, by simply letting $C = 0$, so that also $L_0 = 0$ and $T_0 = 0$. This optimizes stability robustness, but does nothing to improve control system performance, such as its sensitivity and response properties. In Section 5 we introduce an alternative stability robustness criterion that allows consideration of the response properties as well.

It is important to note that although it looks very plausible to characterize the plant perturbations by the bound (12), the bound may in fact allow far more perturbations than may actually occur. By way of example, suppose that the perturbations are caused by variation of a single parameter. Then if these variations have an important effect on the loop gain it may be necessary to choose W quite large to satisfy the bound. This large bound also allows many other perturbations, however, including such that change the order of the plant. Because of this the robustness stability test (14) may easily fail even if the actual parameter perturbations do not destabilize the feedback system.

This phenomenon, usually referred to as conservativeness, seriously handicaps the applicability of the robustness stability analysis described in this section. The model is mainly suited to deal with high-frequency uncertainty caused by parasitic effects and unmodelled dynamics that cause the envelope defined by (12) to be densely filled.

4. A GENERAL PERTURBATION MODEL

In the preceding section we considered perturbations of the form $L_0 \rightarrow L$, where $|L(j\omega) - L_0(j\omega)| / |L_0(j\omega)| \leq |W(j\omega)|$ for all $\omega \in \mathbb{R}$. Equivalently, we may write

$$L_0 \rightarrow L_0(1 + \delta_L W), \tag{16}$$

where δ_L is any frequency dependent function such that $|\delta_L(j\omega)| \leq 1$ for all $\omega \in \mathbb{R}$, that is, such that

$$\|\delta_L\|_\infty \leq 1. \tag{17}$$

This perturbation may be represented as in the block diagram of Fig. 5. Because at this point we are only interested in stability the disturbance has been omitted. The functions W and δ_L are represented as frequency response functions of stable systems.

Figure 5 is a special case of the configuration of Fig. 6, where H represents the dashed block in Fig. 5. In the block diagram of Fig. 6 the perturbation δ is isolated from the rest of the system H .

By the small gain theorem (see for instance Desoer and Vidyasagar, 1975) a sufficient condition for the closed-loop system of Fig. 6 to be stable is that the norm $\|H\delta\|$ of the loop map $H\delta$ be less than 1. By

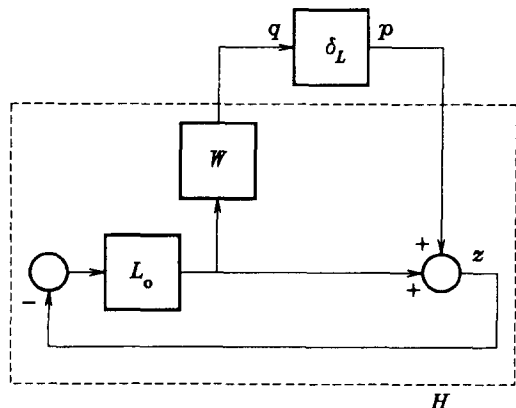


FIG. 5. Feedback loop with perturbation.

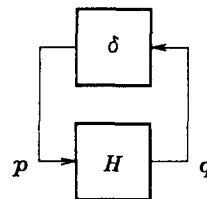


FIG. 6. General perturbation model.

the inequality $\|H\delta\| \leq \|H\| \cdot \|\delta\|$ this is guaranteed if $\|H\| \cdot \|\delta\| < 1$. Taking in particular the ∞ -norm it follows that the perturbed system is stable for all perturbations δ whose ∞ -norm is, at most 1 if

$$\|H\|_\infty < 1. \tag{18}$$

The perturbation model of Fig. 6 with the corresponding condition (18) for stability with respect to all perturbations such that $\|\delta\|_\infty \leq 1$ is simple yet very general. The condition (18) is not only sufficient but also necessary.

To illustrate its application we specialize the result to the configuration of Fig. 5. H is the transfer function from p to q after opening the loop by removing the block “ δ ”. Inspection of Fig. 5 shows that $\hat{z} = \hat{p} - L_0 \hat{z}$, so that

$$\hat{z} = \frac{1}{1 + L_0} \hat{p}. \tag{19}$$

By further inspection we have

$$\hat{q} = -WL_0 \hat{z} = -W \frac{L_0}{1 + L_0} \hat{p} = -WT_0 \hat{p}, \tag{20}$$

so that the transfer function H is given by

$$H = -WT_0. \tag{21}$$

Hence, by (18) stability under perturbation is guaranteed if

$$\|WT_0\|_\infty < 1. \tag{22}$$

This is precisely the stability robustness criterion of Section 3.

The general model of Fig. 6 with the necessary and sufficient condition $\|H\|_\infty < 1$ for robust stability with respect to all perturbations such that $\|\delta\|_\infty \leq 1$ applies to SISO as well as MIMO systems. It was conceived by Doyle (1984). To use the condition for MIMO systems we need discuss how the ∞ -norm is defined for such systems. Consider a stable MIMO system with input u , output y and transfer matrix F as in Fig. 7. The ∞ -norm of the system is the norm induced by the norms

$$\|u\|_2 = \sqrt{\int_{-\infty}^{\infty} u^H(t)u(t) dt},$$

$$\|y\|_2 = \sqrt{\int_{-\infty}^{\infty} y^H(t)y(t) dt}, \tag{23}$$

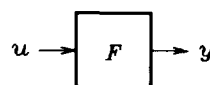


FIG. 7. MIMO system.

of the input and output, respectively. The superscript H denotes the complex conjugate transpose. Again using Parseval's theorem, it may be shown that the norm of the system induced by these signal norms is

$$\|F\|_\infty = \sup_{\omega \in \mathbb{R}} \|F(j\omega)\|_2, \quad (24)$$

where for a constant complex-valued matrix A the notation $\|A\|_2$ indicates the spectral norm

$$\|A\|_2 = \max_i \sigma_i(A), \quad (25)$$

with σ_i the i th singular value \dagger . It follows from (24)–(25) that the ∞ -norm $\|F\|_\infty$ of the stable system with transfer matrix F is found by first computing for each frequency the largest singular value of the frequency response matrix $F(j\omega)$, and then taking the maximum of all these largest singular values over frequency.

In the following section we discuss a further application of the basic stability robustness result.

5. NUMERATOR-DENOMINATOR PERTURBATIONS

In this section we discuss the application of the general stability robustness result to what we call numerator-denominator perturbations, or coprime factor uncertainty, as they are also known. The model may be traced to Vidyasagar (Vidyasagar *et al.*, 1982; Vidyasagar, 1985) and Kwakernaak (1983, 1986). It relies on the representation of the plant transfer function P in the block diagram of Fig. 1 in fractional form as

$$P = \frac{N}{D}. \quad (26)$$

In particular, if P is rational, N obviously can be taken as the numerator polynomial and D as the denominator polynomial. It is not necessary to do this, however, and indeed it sometimes is useful to arrange N and D differently. The numerator-denominator perturbation model represents perturbations in the form

$$P_0 = \frac{N_0}{D_0} \rightarrow P = \frac{N_0 + M\delta_N W_2}{D_0 + M\delta_D W_1}, \quad (27)$$

where the subscripts on N and D denote the nominal system. The terms $M\delta_D W_1$ and $M\delta_N W_2$ model the uncertainty in the denominator and the numerator, respectively. The frequency dependent functions MW_1 and MW_2 represent the largest possible perturbations of the denominator and numerator, respectively, and δ_D and δ_N are frequency dependent functions of magnitude not greater than one. The factor M is included for added flexibility. Its use (for partial pole placement) becomes clear in Section 6.

\dagger If A is an $n \times m$ matrix, the singular values of A are the $\min(n, m)$ largest of the m nonnegative numbers $\sqrt{\lambda_i(A^H A)}$, $i = 1, 2, \dots, m$. Here λ_i denotes the i th eigenvalue. The singular values are also the $\min(n, m)$ largest of the n numbers $\sqrt{\lambda_i(A A^H)}$, $i = 1, 2, \dots, n$.

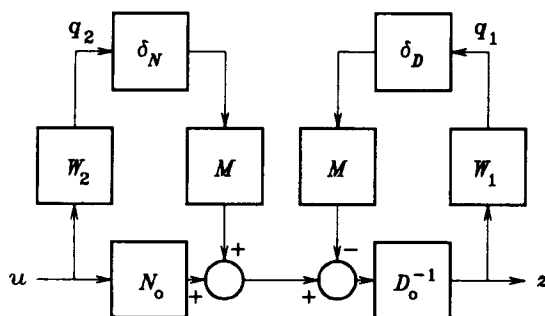


FIG. 8. Numerator-denominator perturbation model.

It is not difficult to check that the perturbation (27) may be represented as in the block diagram of Fig. 8. Note that the perturbation δ_D appears in a feedback loop. Including the plant in the control system configuration of Fig. 1 the block diagram may be arranged as in Fig. 9, where the block “ δ_P ” is described by

$$\hat{p} = -\delta_D \hat{q}_1 + \delta_N \hat{q}_2 = \underbrace{\begin{bmatrix} -\delta_D & \delta_N \end{bmatrix}}_{\delta_P} \underbrace{\begin{bmatrix} \hat{q}_1 \\ \hat{q}_2 \end{bmatrix}}_{\hat{q}}. \quad (28)$$

The dashed lines in Fig. 9 indicate how the situation may be reduced to the perturbation model of Fig. 6. For the application of condition (18) for robust stability we need to assume that the closed-loop system is stable, and that moreover M , W_1 , and W_2 have all their poles in the open left-half plane.

The block marked “ H ” has input p and output $q = \text{col}(q_1, q_2)$. To find the transfer matrix H , we first inspect Fig. 9 to establish the signal balance equation $\hat{z} = D_0^{-1}(M\hat{p} - N_0 C \hat{z})$. It follows that

$$\hat{z} = \frac{D_0^{-1} M}{1 + D_0^{-1} N_0 C} \hat{p} = \frac{V}{1 + P_0 C} \hat{p}, \quad (29)$$

where we define $V = D_0^{-1} M$. By further inspection we see that

$$\begin{aligned} \hat{q}_1 &= W_1 \hat{z} = \frac{W_1 V}{1 + P_0 C} \hat{p} = W_1 S_0 V \hat{p}, \\ \hat{q}_2 &= -W_2 C \hat{z} = -\frac{W_2 C V}{1 + P_0 C} \hat{p} = -W_2 U_0 V \hat{p}, \end{aligned} \quad (30)$$

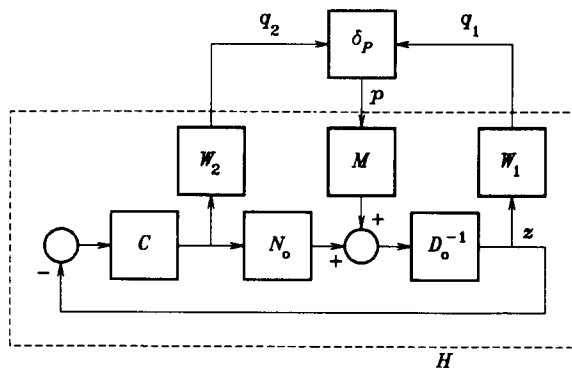


FIG. 9. Numerator-denominator perturbation model in feedback loop.

where

$$S_0 = \frac{1}{1 + P_0 C}, \quad U_0 = \frac{C}{1 + P_0 C}, \quad (31)$$

are the nominal sensitivity function and the nominal input sensitivity function, respectively, of the feedback system. The input sensitivity function U is the transfer function from the disturbance to the plant input. It is related to the complementary sensitivity function T as $T = PU$.

From (30) we see that the transfer matrix H in Fig. 9 is given by

$$H = \begin{bmatrix} W_1 S_0 V \\ -W_2 U_0 V \end{bmatrix}. \quad (32)$$

It is easy to check that the 1×2 matrix $A = [A_1 \ A_2]$ has the single singular value $\sqrt{|A_1|^2 + |A_2|^2}$. Hence, the square of the ∞ -norm of the perturbation $\delta_p = [-\delta_D \ \delta_N]$ is

$$\|\delta\|_\infty^2 = \sup_{\omega \in \mathbb{R}} (|\delta_D(j\omega)|^2 + |\delta_N(j\omega)|^2). \quad (33)$$

The 2×1 matrix $A = [A_1 \ A_2]^T$ also has the single singular value $\sqrt{|A_1|^2 + |A_2|^2}$. Hence, the square of the ∞ -norm of the system with transfer matrix H as given by (32) is

$$\|H\|_\infty^2 = \sup_{\omega \in \mathbb{R}} (|W_1(j\omega)S_0(j\omega)V(j\omega)|^2 + |W_2(j\omega)U_0(j\omega)V(j\omega)|^2). \quad (34)$$

It follows that the closed-loop system is stable for all numerator-denominator perturbations $\delta_p = [-\delta_D \ \delta_N]$ satisfying the bound

$$|\delta_D(j\omega)|^2 + |\delta_N(j\omega)|^2 \leq 1, \quad \text{for all } \omega \in \mathbb{R}, \quad (35)$$

if and only if the sensitivity function S_0 and the input sensitivity function U_0 satisfy the inequality

$$\|W_1(j\omega)S_0(j\omega)V(j\omega)\|^2 + \|W_2(j\omega)U_0(j\omega)V(j\omega)\|^2 < 1, \quad (36)$$

for all $\omega \in \mathbb{R}$.

Alternative interpretation

It is useful to consider an alternative interpretation of this stability robustness result. For the numerator-

denominator perturbation model (27) the relative perturbation of the denominator is given by

$$\frac{D - D_0}{D_0} = \frac{M\delta_D W_1}{D_0} = V W_1 \delta_D = w_1 \delta_D, \quad (37)$$

where $w_1 = V W_1$. Similarly, the relative perturbation of the numerator is

$$\frac{N - N_0}{N_0} = \frac{M\delta_N W_2}{N_0} = \frac{V W_2}{P_0} \delta_N = w_2 \delta_N, \quad (38)$$

where $w_2 = W_2 V / P_0$. From (35) it follows with (37)-(38) that we consider perturbations satisfying

$$\left| \frac{D - D_0}{D_0} \right|_{w_1}^2 + \left| \frac{N - N_0}{N_0} \right|_{w_2}^2 \leq 1, \quad (39)$$

on the imaginary axis. Substituting $W_1 V = w_1$ and $W_2 V = w_2 P_0$ into (36) we see that the system is robustly stable for such perturbations if and only if

$$|S_0 w_1|^2 + |T_0 w_2|^2 < 1, \text{ on the imaginary axis,} \quad (40)$$

since $P_0 U_0 = T_0$.

By (39), the functions w_1 and w_2 are measures for the relative sizes of the perturbations in the denominator and the numerator of the plant transfer matrix P , respectively. The stability robustness test (40) then indicates that the nominal sensitivity function S_0 should be small for those frequencies where the relative perturbations in the denominator are large, and that the nominal complementary sensitivity function T_0 should be small for those frequencies where the relative perturbations in the numerator are large.

Conversely, this interpretation provides us with an indication how to model perturbations compatibly with performance requirements. Customary performance specifications require the sensitivity function to be small at low frequencies, and to level off to one at high frequencies (see Fig. 10). Designing the system

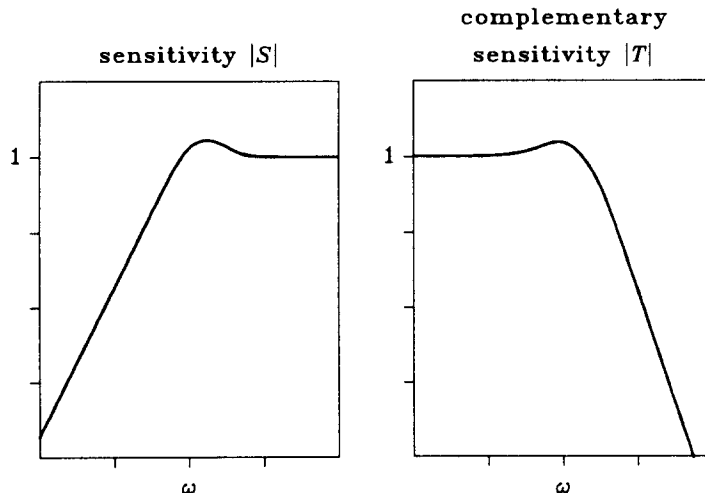


FIG. 10. Bode magnitude plots of typical sensitivity and complementary sensitivity functions.

this way ensures disturbance attenuation over the widest possible frequency range given the plant capacity (that is, given the largest inputs the plant can absorb).

This means that low-frequency perturbations are best modeled as denominator perturbations. The most important low-frequency perturbations are normally caused by parameter uncertainty, often referred to as structured uncertainty. On the other hand, high-frequency perturbations are best modeled as numerator perturbations, because (complementarily—see Fig. 10) the complementary sensitivity function T_0 is small at high frequencies. High-frequency perturbations are usually caused by parasitic effects and unmodeled dynamics, often known as unstructured uncertainty.

The examples in Sections 7 and 8 illustrate the application of these ideas.

6. THE MIXED SENSITIVITY PROBLEM

In Section 5 it was found that stability robustness with respect to numerator–denominator perturbations such that

$$|\delta_D(j\omega)|^2 + |\delta_N(j\omega)|^2 \leq 1, \quad \omega \in \mathbb{R}, \quad (41)$$

is guaranteed if $\|H\|_\infty < 1$, where (omitting the subscripts on S and U)

$$\|H\|_\infty^2 = \sup_{\omega \in \mathbb{R}} (|W_1(j\omega)S(j\omega)V(j\omega)|^2 + |W_2(j\omega)U(j\omega)V(j\omega)|^2). \quad (42)$$

Given a feedback system with compensator C that does not satisfy this inequality one may look for a different compensator that does achieve inequality. An effective way of doing this is to consider the problem of minimizing $\|H\|_\infty$ with respect to all compensators C that stabilize the system. If the minimal value of $\|H\|_\infty$ is greater than 1, no compensator exists that stabilizes the systems for all perturbations satisfying (41). In this case, stability robustness is only obtained for perturbations satisfying (41) with the right-hand side replaced with $1/\lambda^2$.

The problem of minimizing

$$\left\| \begin{bmatrix} W_1 S V \\ W_2 U V \end{bmatrix} \right\|_\infty, \quad (43)$$

(Kwakernaak, 1983, 1985) is a version of what is known as the mixed sensitivity problem (Verma and Jonckheere, 1984). The name derives from the fact that the optimization involves both the sensitivity and the input sensitivity function (or, in other versions, the complementary sensitivity function).

In what follows we explain that the mixed sensitivity problem cannot only be used to verify stability robustness for a class of perturbations, but also to achieve a number of important design targets for the one-degree-of-freedom feedback configuration of Fig. 1.

Frequency response shaping

The mixed sensitivity problem may be used for performance design by shaping the sensitivity and input sensitivity functions. The reason is that the

solution of the mixed sensitivity problem has the property that the frequency dependent function

$$|W_1(j\omega)S(j\omega)V(j\omega)|^2 + |W_2(j\omega)U(j\omega)V(j\omega)|^2, \quad (44)$$

whose peak value is minimized, actually is a constant (Kwakernaak, 1985). This is known as the equalizing property. If we denote the constant as λ^2 , with λ nonnegative, it immediately follows from

$$|W_1(j\omega)S(j\omega)V(j\omega)|^2 + |W_2(j\omega)U(j\omega)V(j\omega)|^2 = \lambda^2, \quad (45)$$

that for the optimal solution

$$\begin{aligned} |W_1(j\omega)S(j\omega)V(j\omega)|^2 &\leq \lambda^2, & \omega \in \mathbb{R}, \\ |W_2(j\omega)U(j\omega)V(j\omega)|^2 &\leq \lambda^2, & \omega \in \mathbb{R}. \end{aligned} \quad (46)$$

Hence,

$$|S(j\omega)| \leq \frac{\lambda}{|W_1(j\omega)V(j\omega)|}, \quad \omega \in \mathbb{R}, \quad (47)$$

$$|U(j\omega)| \leq \frac{\lambda}{|W_2(j\omega)V(j\omega)|}, \quad \omega \in \mathbb{R}. \quad (48)$$

By choosing the functions, W_1 , W_2 , and V suitably S and U may be made small in appropriate frequency regions.

If the weighting functions are appropriately chosen (in particular, with W_1V large at low frequencies and W_2V large at high frequencies) often the solution of the mixed sensitivity problem has the property that the first term of the criterion dominates at low frequencies and the second at high frequencies:

$$\underbrace{|W_1(j\omega)S(j\omega)V(j\omega)|^2}_{\text{dominates at low frequencies}} + \underbrace{|W_2(j\omega)U(j\omega)V(j\omega)|^2}_{\text{dominates at high frequencies}} = \lambda^2 \quad (49)$$

As a result,

$$|S(j\omega)| \approx \frac{\lambda}{|W_1(j\omega)V(j\omega)|}, \quad \text{for } \omega \text{ small}, \quad (50)$$

$$|U(j\omega)| \approx \frac{\lambda}{|W_2(j\omega)V(j\omega)|}, \quad \text{for } \omega \text{ large}. \quad (51)$$

This allows quite effective control over the shape of the sensitivity and input sensitivity functions, and, hence, over the performance of the feedback system.

Type k control and high-frequency roll-off

In (50)–(51), equality may often be achieved asymptotically. Suppose that $|W_1(j\omega)V(j\omega)|$ behaves as $1/\omega^k$ as $\omega \rightarrow 0$. This is the case if $W_1(s)V(s)$ includes a factor s^k in the denominator. Then $|S(j\omega)|$ behaves as ω^k as $\omega \rightarrow 0$, which implies a type k control system, with excellent low-frequency disturbance attenuation if $k \geq 1$. If $k = 1$, the system has an integrating action.

Likewise, suppose that $|W_2(j\omega)V(j\omega)|$ behaves as ω^m as $\omega \rightarrow \infty$. This is the case if W_2V is nonproper, that is, if the degree of the numerator exceeds that of the denominator (by m). Then $|U(j\omega)|$ behaves as ω^{-m} as $\omega \rightarrow \infty$. From $U = -C/(1 + PC)$ it follows that

$C = -U/(1 + UP)$. Hence, if P is strictly proper and $m \geq 0$, also C behaves as ω^{-m} , and $T = PC/(1 + PC)$ behaves as $\omega^{-(m+e)}$, with e the pole excess of P . This means that by choosing m we pre-assign the high-frequency roll-off of the compensator transfer function, and that of the complementary and input sensitivity functions. This is important for robustness against high-frequency unstructured plant perturbations.

Partial pole placement

There is a further important property of the solution of the mixed sensitivity problem that needs to be discussed before considering an example. This concerns a pole cancellation phenomenon that is sometimes misunderstood. First note that the equalizing property implies that

$$W_1(s)W_1(-s)S(s)S(-s)V(s)V(-s) + W_2(s)W_2(-s)U(s)U(-s)V(s)V(-s) = \lambda^2, \quad (52)$$

for all s in the complex plane. Next we write the transfer function P and the weighting functions W_1 , W_2 , and V in rational form as

$$P = \frac{N}{D}, \quad W_1 = \frac{A_1}{B_1}, \quad W_2 = \frac{A_2}{B_2}, \quad V = \frac{M}{E}, \quad (53)$$

with all numerators and denominators polynomials. Note that at this point we do not necessarily take the denominator of V equal to D as before. Then if the compensator transfer function is represented in rational form as $C = Y/X$ it easily follows that

$$S = \frac{DX}{DX + NY}, \quad U = \frac{DY}{DX + NY}. \quad (54)$$

The denominator

$$D_{cl} = DX + NY, \quad (55)$$

is the closed-loop characteristic polynomial of the feedback system. Substituting S and U we easily obtain from (52) that

$$\frac{D^-D \cdot M^-M \cdot (A_1^-A_1B_2^-B_2X^-X + A_2^-A_2B_1^-B_1Y^-Y)}{E^-E \cdot B_1^-B_1 \cdot B_2^-B_2 \cdot D_{cl}^-D_{cl}} = \lambda^2, \quad (56)$$

where if A is any rational or polynomial function, A^- is defined by $A^-(s) = A(-s)$.

Since the right-hand side of (56) is a constant, all factors in the numerator of the rational function on the left cancel against corresponding factors in the denominator. In particular, the factor D^-D cancels. If there are no cancellations between D^-D and $E^-EB_1^-B_1B_2^-B_2$, the closed-loop characteristic polynomial D_{cl} (which by stability has left-half plane roots only) necessarily has among its roots the roots of D , where any roots of D in the right-half plane are mirrored into the left-half plane.

This means that the open-loop poles (the roots of D), possibly after having been mirrored into the left-half plane, reappear as closed-loop poles. This phenomenon, which is not propitious for a good design, may be avoided, and indeed, turned into an

advantage, by choosing the denominator polynomial E of V equal to the plant denominator polynomial D , so that

$$V = \frac{M}{D}. \quad (57)$$

With this special choice of the denominator of V , the polynomial E cancels against D in (56), so that the open-loop poles do not reappear as closed-loop poles.

Further inspection of (56) shows that if there are no cancellations between M^-M and $E^-EB_1^-B_1B_2^-B_2$, and we assume without loss of generality that M has left-half plane roots only, the polynomial M cancels against a corresponding factor in D_{cl} . If we take V proper (which ensures $V(j\omega)$ to be finite at high frequencies) the polynomial M has the same degree as D , and, hence, the same number of roots as D . This means that choosing M is equivalent to reassigning the open-loop poles (the roots of D) to the locations of the roots of M . By suitably choosing the remaining weighting functions W_1 and W_2 these roots may often be arranged to be the dominant poles.

This technique, known as partial pole placement (Kwakernaak, 1986; Postlethwaite *et al.*, 1990), allows further control over the design. It is very useful in designing for a given bandwidth and good time response properties.

In the design examples in Sections 7 and 8 it is illustrated how the ideas of partial pole placement and frequency shaping are combined.

A fuller account of pole-zero cancellation phenomena in \mathcal{H}_∞ -optimization problems is given by Sefton and Glover (1990).

Design for robustness

As we have seen, the mixed sensitivity problem is a promising tool for frequency response shaping. By appropriate choices of the functions V , W_1 , and W_2 , the sensitivity function may be made small at low frequencies and the input sensitivity function (or equivalently, the complementary sensitivity function) small at high frequencies. These are necessary requirements for the system to perform adequately, that is, to attenuate disturbances sufficiently given the plant capacity and presence of measurement noise.

On the other hand, as seen at the end of Section 5, a small sensitivity function S at low frequencies provides robustness against low-frequency perturbations in the plant denominator while a small complementary sensitivity function T at high frequencies protects against high-frequency perturbations in the plant numerator. Investigation of the low-frequency behavior of S and the high-frequency behavior of T permits to estimate the maximal size of the allowable perturbations. Conversely, any information that is available about the size of the perturbations may be used to select the weighting functions V , W_1 and W_2 . The choice of these functions generally involves considerations about both performance and robustness. These design targets are not necessarily incompatible or competitive.

It is clear that the crossover region is critical for robustness. The crossover region is the frequency

region where the magnitude of the loop gain $L = PC$ —which generally is large for low frequencies and small for high frequencies—crosses over from values greater than 1 to values less than 1. In this region, neither the sensitivity function nor the complementary sensitivity function is small.

Only for minimum-phase plants—that is, plants whose poles and zeros are all in the left-half plane—the sensitivity and complementary sensitivity functions can be molded more or less at will. The presence of right-half plane zeros or poles imposes important constraints. Right-half plane zeros constrain the bandwidth below which effective disturbance attenuation is possible, that is, for which S can be made small. In fact, the largest achievable bandwidth is determined by the right-half plane zero closest to the origin. Right-half plane poles limit the bandwidth of the complementary sensitivity function T , that is, the frequency above which T starts to roll off. Here, the smallest possible bandwidth is determined by the right-half plane pole furthest from the origin. If the plant has both right-half plane poles and right-half plane zeros the difficulties are aggravated. Especially if the right-half plane poles and zeros are close considerable peaking of the sensitivity and complementary sensitivity functions occurs.

These results are discussed at length by Engell (1988) for the SISO case and Freudenberg and Looze (1988) for the scalar and multivariable cases. The results show that plants with right-half plane poles and zeros have serious robustness handicaps.

7. EXAMPLE 1: DOUBLE INTEGRATOR

In this section we illustrate the application of the mixed sensitivity problem to a textbook style design example that is simple enough to be completely transparent. Consider a SISO plant with nominal transfer function

$$P_0(s) = \frac{1}{s^2}. \quad (58)$$

The actual, perturbed plant has the transfer function

$$P(s) = \frac{g}{s^2(1+s\theta)}, \quad (59)$$

where g is nominally one and the parasitic time constant θ is nominally 0.

We start with a preliminary robustness analysis. The variations in the parasitic time constant θ mainly cause high-frequency perturbations, while the low-frequency perturbations are primarily the effect of the variations in the gain g . Accordingly, we model the effect of the time constant as a numerator perturbation, and the gain variations as denominator perturbations, and write

$$P(s) = \frac{1}{\frac{1+s\theta}{g} s^2}. \quad (60)$$

Correspondingly, the relative perturbations of the

denominator and the numerator are

$$\frac{D(s) - D_0(s)}{D_0(s)} = \frac{1}{g} - 1, \quad (61)$$

$$\frac{N(s) - N_0(s)}{N_0(s)} = \frac{-s\theta}{1+s\theta}. \quad (62)$$

The relative perturbation (61) of the denominator is constant over all frequencies, hence also in the crossover region. Because the plant is minimum-phase, trouble-free crossover may be achieved (that is, without undue peaking of the sensitivity and complementary sensitivity functions) and, hence, we expect that—in the absence of other perturbations—variations in $|1/g - 1|$ up to almost 1 will be tolerated.

The size of the relative perturbation (62) of the numerator is less than 1 for frequencies below $1/\theta$, and equal to 1 for high frequencies. To prevent destabilization it is advisable to make the complementary sensitivity small for frequencies greater than $1/\theta$. As the complementary sensitivity starts to decrease at the closed-loop bandwidth, the largest possible value of θ dictates the bandwidth. Assuming that performance requirements specify the system to have a closed-loop bandwidth of 1, we expect that—in the absence of other perturbations—values of the parasitic time constant θ up to 1 will not destabilize the system.

Thus, both for robustness and performance, we aim at a closed-loop bandwidth of 1 with small sensitivity at low frequencies and a sufficiently fast decrease of the complementary sensitivity at high frequencies with a smooth transition in the crossover region. To accomplish this with a mixed sensitivity design, we successively consider the choice of the functions $V = M/D$ (that is, of the polynomial M), W_1 and W_2 .

To obtain a good time response corresponding to the bandwidth 1, which does not suffer from sluggishness or excessive overshoot, we assign two dominant poles to the locations $\frac{1}{2}\sqrt{2}(-1 \pm j)$. This is achieved by choosing the polynomial M as

$$\begin{aligned} M(s) &= [s - \frac{1}{2}\sqrt{2}(-1 + j)][s - \frac{1}{2}\sqrt{2}(-1 - j)] \\ &= s^2 + s\sqrt{2} + 1, \end{aligned} \quad (63)$$

so that

$$V(s) = \frac{s^2 + s\sqrt{2} + 1}{s^2}. \quad (64)$$

We choose the weighting function W_1 equal to 1. Then if the first of the two terms of the mixed sensitivity criterion dominates at low frequencies we have $|S| \approx |\lambda|/|VW_1|$, or

$$|S(j\omega)| \approx |\lambda| \left| \frac{(j\omega)^2}{(j\omega)^2 + j\omega\sqrt{2} + 1} \right|, \quad (65)$$

at low frequencies. Figure 11 shows the Bode magnitude plot of the factor $1/V$, which implies a very good low-frequency behavior of the sensitivity function. Owing to the presence of the double open-loop pole at the origin the feedback system is of type 2.

Next contemplate the high-frequency behavior. For high frequencies V is constant and equal to 1.

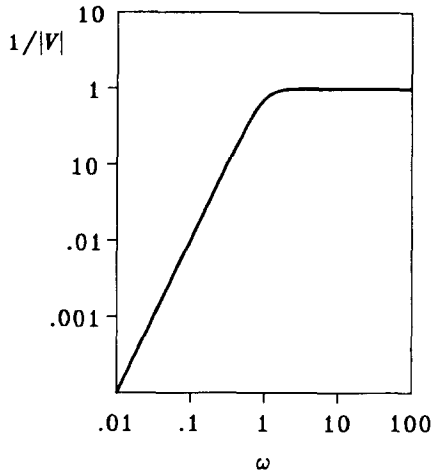


FIG. 11. Bode magnitude plot of $1/V$.

Consider choosing W_2 as

$$W_2(s) = c(1 + rs), \tag{66}$$

with c and r nonnegative constants such that $c \neq 0$. Then for high frequencies the magnitude of W_2 asymptotically behaves as c if $r=0$, and as $cr\omega$ if $r \neq 0$.

Hence, if $r=0$, the high-frequency roll-off of the input sensitivity function U and the compensator transfer function C is 0 and that of the complementary sensitivity T is 2 decades/decade (40 dB/decade).

If $r \neq 0$, U and C roll off at 1 decade/decade (20 dB/decade), and T rolls off at 3 decades/decade (60 dB/decade).

We first study the case $r=0$, which results in a proper but not strictly proper compensator transfer function C , and a high-frequency roll-off of T of 2 decades/decade. Figure 12 shows the sensitivity function S and the complementary sensitivity function T for $c=1/100$, $c=1/10$, $c=1$, and $c=10$. Inspection shows that as c increases, $|T|$ decreases and $|S|$ increases, which conforms to expectation. The

smaller c is, the closer the shape of $|S|$ is to that of Fig. 11.

We choose $c=1/10$. This makes the sensitivity small with little peaking at the cut-off frequency. The corresponding optimal compensator has the transfer function

$$C(s) = 1.2586 \frac{s + 0.61967}{1 + 0.15563s}, \tag{67}$$

and results in the closed-loop poles $\frac{1}{2}\sqrt{2}(-1 \pm j)$ and -5.0114 . The two former poles dominate the latter pole, as planned. The minimal ∞ -norm is $\|H\|_\infty = 1.2861$.

Robustness against high-frequency perturbations may be improved by making the complementary sensitivity function T decrease faster at high frequencies. This is accomplished by taking the constant r nonzero. Inspection of W_2 as given by (66) shows that by choosing $r=1$ the resulting extra roll-off of U , C , and T sets in at the frequency 1. For $r=1/10$ the break point is shifted to the frequency 10. Figure 13 shows the resulting magnitude plots. For $r=1/10$ the sensitivity function has little extra peaking while starting at the frequency 10 the complementary sensitivity function rolls off at a rate of 3 decades/decade. The corresponding optimal compensator transfer function is

$$C(s) = 1.2107 \frac{s + 0.5987}{1 + 0.20355s + 0.01267s^2}, \tag{68}$$

which results in the closed-loop poles $\frac{1}{2}\sqrt{2}(-1 \pm j)$ and $-7.3281 \pm j1.8765$. Again the former two poles dominate the latter. The minimal ∞ -norm is $\|H\|_\infty = 1.3833$.

Inspection of the two compensators (67) and (68) shows that both basically are PD compensators with high-frequency roll-off. The optimal compensators were computed using a MATLAB package for the solution of \mathcal{H}_∞ -optimization problems (Kwakernaak, 1990b) based on the polynomial method of Section 10.

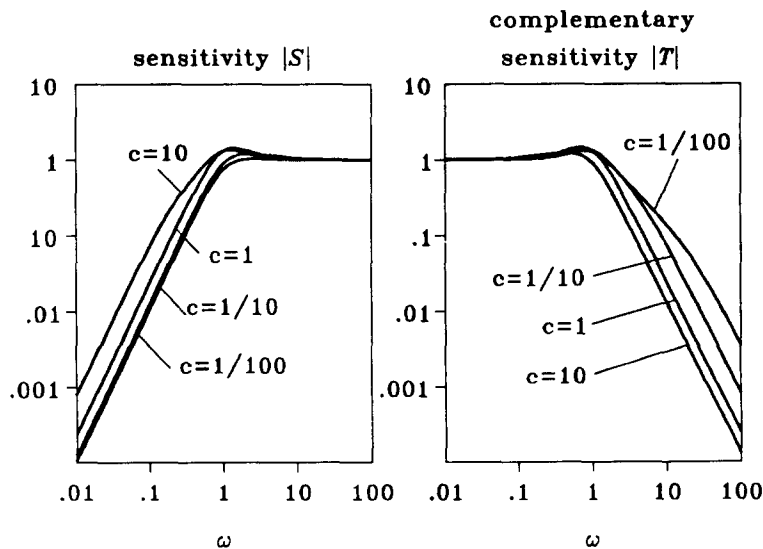


FIG. 12. Bode magnitude plots of S and T for $r=0$.

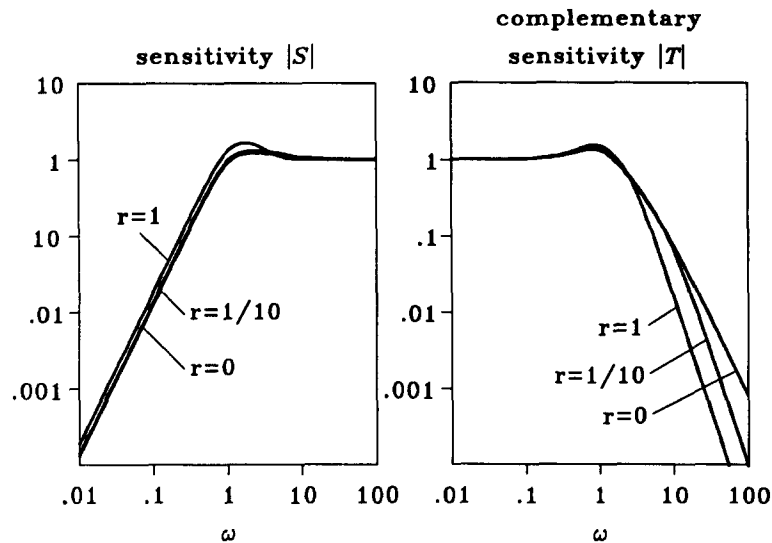
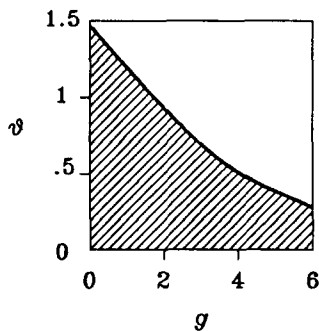
FIG. 13. Bode magnitude plots of S and T for $c = 1/10$.

FIG. 14. Stability region.

We conclude this example with a brief analysis to check whether our expectations about robustness have come true. Given the compensator $C = Y/X$ the closed-loop characteristic polynomial of the perturbed plant is $D(s)X(s) + N(s)Y(s) = (1 + s\theta)s^2X(s) + gY(s)$. By straightforward root locus computation,† which involves fixing one of the two parameters g and θ and varying the other, the stability region of Fig. 14 may be established for the compensator (67). That for the other compensator is similar. The diagram shows that for $\theta = 0$ the closed-loop system is stable for all $g > 0$, that is, for all $-1 < 1/g - 1 < \infty$. This stability interval is larger than predicted. For $g = 1$ the system is stable for $0 \leq \theta < 1.179$, which also is a somewhat larger interval than expected.

8. EXAMPLE 2: SHIP COURSE CONTROL

In this section we discuss a more concrete design problem. It deals with the heading control of a ship moving at constant velocity, and is included in the 1990 IFAC Benchmark Problems for Control System Design (Åström, 1990). Our presentation is related to the discussion in a recent doctoral dissertation by

† At the suggestion of one of the reviewers. The author is indebted to this and the other reviewers for many positive and constructive comments.

TABLE 1. PARAMETER VALUES FOR THE SHIP TRANSFER FUNCTION

Operating conditions	b_0	b_1	a_0	a_1
"Nominal"	0.98	1.72	2.13	-0.325
1	1.07	0.75	1.96	-0.70
2	1.05	0.74	1.66	-0.59
3	0.93	0.85	1.86	-0.47
4	0.71	1.29	2.02	-0.21
5	0.89	1.83	2.35	0.05

Lundh (1991). The ship transfer function from the rudder angle to the yaw angle is

$$P(s) = \frac{(b_0s + 1)b_1}{s(s + a_0)(s + a_1)}, \quad (69)$$

where the values of the parameters b_0 , b_1 , a_0 , and a_1 , depend upon the operating conditions, including speed, trim, and loading. In Table 1 the parameter values are given for five operating conditions. The table also includes a set of values that were chosen to represent the "nominal" plant. The table shows that the sign of the pole a_1 depends on the operating conditions, so that the number of unstable open-loop poles is not constant. Lundh (1991) formulates the following design specifications:

- (1) constant load disturbances at the plant input are rejected at the output;
- (2) the closed-loop system is stable at all operating conditions.

We first discuss requirement 1, that constant input load disturbances be rejected. In the configuration of Fig. 1 the transfer function from a load disturbance that is additive to the plant input to the control system output z is

$$R = \frac{P}{1 + PC} = \frac{NX}{DX + NY}, \quad (70)$$

where we write $P = N/D$, $C = Y/X$. Inspection shows that for constant input load rejection the denominator

polynomial X of the compensator needs to contain a factor s , that is, the compensator should have integrating action.

Another way of looking at this requirement is to recognize that the transfer function R is related to the sensitivity function S as $R = PS$. For low frequencies the ship transfer function P is proportional to $1/s$. Hence, for R to behave as s , the sensitivity function S should behave as s^2 at low frequencies. In view of the asymptotic analysis of Section 6 this means that the product of weighting functions W_1V should behave as $1/s^2$. In Section 6 we chose $V = M/D$, $W_1 = A_1/B_1$. For the example at hand, D contains a factor s , so that V already has this factor in the denominator. To provide the additional factor s needed in the denominator of W_1V we modify the weighting function W_1 to

$$W_1(s) = \frac{\omega_1 + s}{s} \bar{W}_1(s), \quad (71)$$

with ω_1 the frequency up to which the effect of the integrating action extends. \bar{W}_1 provides further freedom in selecting W_1 . This technique of choosing W_1 to provide integrating action in the compensator also applies to other examples.

Next we discuss the stability robustness specification 2. Since we plan to use the mixed sensitivity design method, we consider which perturbations should be assigned to the plant numerator and which to the denominator. Obviously, the perturbation that causes poles to cross the imaginary axis, that is, the perturbations in the parameter a_1 , should be relegated to the denominator. The perturbations in the gain parameter b_1 strongly affect the low-frequency plant characteristics, and therefore are also included in the denominator perturbations. The variations in b_0 principally affect the high-frequency characteristics and therefore are included in the numerator perturbations. The variations in the far-away pole a_0 are mainly important for the high-frequency behavior, but because of the way the pole enters P it also affects the gain. We therefore write the transfer function P in the form

$$P(s) = \frac{b_0s + 1}{\frac{a_0}{b_1}s \left(\frac{s}{a_0} + 1 \right) (s + a_1)} = \frac{b_0s + 1}{\beta_1s(\alpha_0s + 1)(s + a_1)}, \quad (72)$$

where

$$\alpha_0 = \frac{1}{a_0}, \quad \beta_1 = \frac{a_0}{b_1}. \quad (73)$$

Including the variation of α_0 in the numerator perturbations we thus rewrite the plant transfer function as

$$P(s) = \frac{N(s)}{D(s)} = \frac{\frac{b_0s + 1}{\alpha_0s + 1} (\bar{\alpha}_0s + 1)}{\beta_1(s + a_1)(\bar{\alpha}_0s + 1)}, \quad (74)$$

where the overbar denotes the nominal value.

It is easy to find that the relative perturbations of

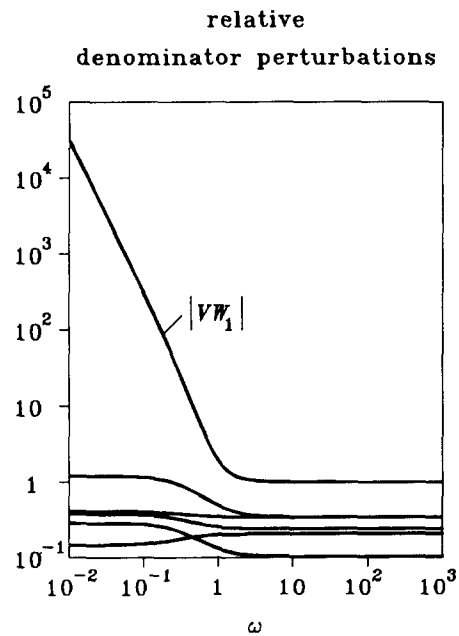


FIG. 15. Magnitudes of relative denominator perturbations for the ship transfer function.

the denominator may be expressed as

$$\frac{D(s) - D_0(s)}{D_0(s)} = \frac{(\beta_1 - \bar{\beta}_1)s + (a_1\beta_1 - a_1\bar{\beta}_1)}{\bar{\beta}_1(s + \bar{a}_1)}, \quad (75)$$

with the overbars again denoting nominal values. Figure 15 displays magnitude plots of the relative perturbations for the various parameter combinations of Table 1. We establish a bound for the perturbations in a suitable form. As a preamble to this, we note from Fig. 15 that above the frequency 1 the relative denominator perturbations are less than 1. For this reason, we aim at a closed-loop bandwidth of about 1.

From (37) we see that at low frequencies the relative denominator perturbations need to be bounded by

$$\left| \frac{D - D_0}{D_0} \right| \leq |VW_1|. \quad (76)$$

Choosing W_1 as in (71), with $\bar{W}_1(s) = 1$, we consider

$$V(s)W_1(s) = \frac{M(s)}{\bar{\beta}_1s(s + \bar{a}_1)(\bar{\alpha}_0s + 1)} \frac{\omega_1 + s}{s}, \quad (77)$$

with M a polynomial of degree 3 to be chosen, and ω_1 a constant to be selected. M and ω_1 should be determined such that, first, the bound (76) holds. Second, while doing this we need to remember that the roots of M reappear as closed-loop poles. Third, the constant ω_1 delimits the frequency interval over which the integrating action extends. We choose $\omega_1 = 1$, in line with our decision to choose the closed-loop bandwidth equal to 1. Furthermore, we choose one of the roots of M as $-\bar{a}_0 = -2.13$. This means that the open-loop faraway nominal pole at -2.13 is left in place. Next, we place the two remaining poles of M in a second-order Butterworth configuration with radius 1, that is, we choose this pole pair as $\frac{1}{\sqrt{2}}(-1 \pm j)$. The choice of the radius is

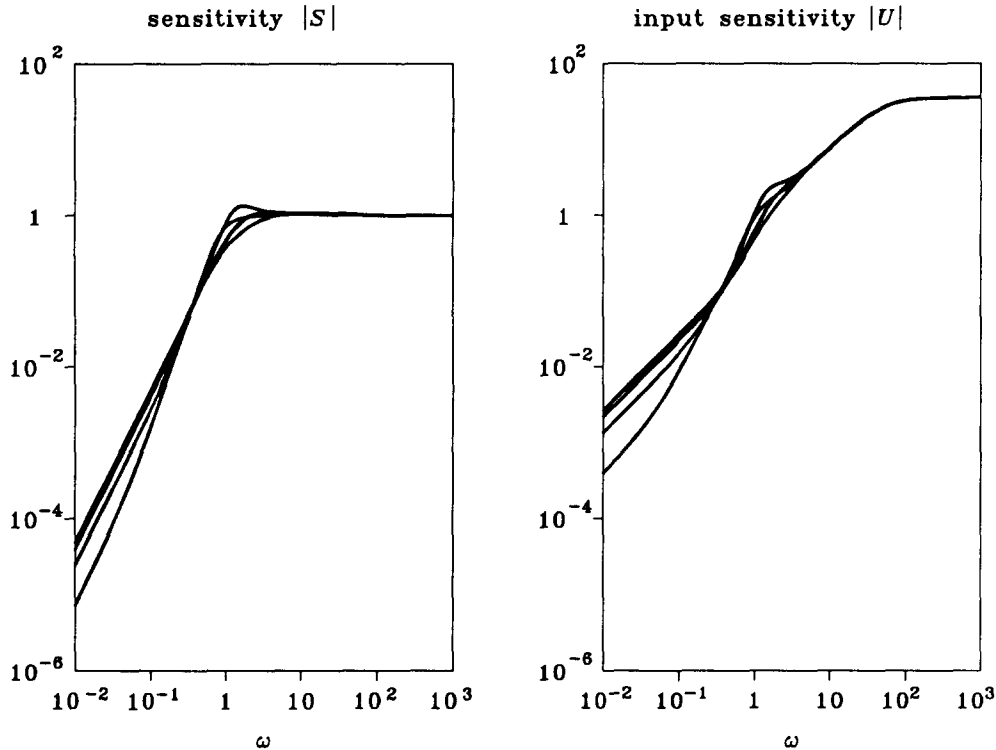


FIG. 16. Magnitudes of the sensitivity and input sensitivity for the ship controller design.

again governed by the selection of a closed-loop bandwidth 1. Finally, for normalization we provide M with a leading coefficient such that $V(\infty)W_1(\infty) = 1$.

Thus, we let

$$M(s) = \beta_1(s^2 + \sqrt{2}s + 1)(s - \bar{a}_0). \quad (78)$$

Figure 15 includes a plot of the magnitude of VW_1 . If this magnitude is a bound for the relative denominator perturbations the closed-loop system is robustly stabilized if the minimal value of the mixed sensitivity criterion is less than 1. If the minimal value λ is greater than 1, the bound needs to be rescaled to VW_1/λ . For the plant at hand, which has no right-half plane zeros, and given the normalization $V(\infty)W_1(\infty) = 1$, from experience it may be expected that the minimal value λ is somewhat larger than 1, say, between 1 and 2. Figure 15 shows that a margin of this order of magnitude is available.

The next logical step is to analyse the numerator perturbations. A cursory exploration that is not reproduced here indicates that the numerator perturbations present no great danger to stability robustness.

The final step in the preparation of the mixed sensitivity procedure is to choose the weighting function W_2 . Choosing W_2 constant is expected to make the compensator transfer function proper but not strictly proper. In view of the normalization $V(\infty)W_1(\infty) = 1$, we tentatively let $W_2(s) = 0.01$.

Solution of the mixed sensitivity problem results in a minimal ∞ -norm of $\lambda = 1.0607$. The optimal compensator transfer function is given by

$$C(s) = \frac{0.5468(s + 2.1277)((s + 0.4331)^2 + 0.4098^2)}{s(s + 47.9401)(s + 1.0204)}. \quad (79)$$

C has a pole at 0, as expected, and the transfer function is proper but not strictly proper, as predicted. The nominal closed-loop poles are -45.2010 , -2.1277 , $-0.7071 \pm j0.7071$, -1.0173 , and -1.0030 . They include the pre-assigned poles -2.1277 and $-0.7071 \pm j0.7071$. It may be checked by direct computation of the closed-loop poles that the feedback system remains stable, with good stability margins, at all operating points. Figure 16 shows plots of the magnitudes of the sensitivity function S and the input sensitivity function U for the various operating points.

For improved robustness against high-frequency unstructured uncertainty it is necessary to make the compensator strictly proper to provide roll-off of the complementary sensitivity T and the input sensitivity U . To accomplish this we modify the weighting function W_2 to

$$W_2(s) = 0.01 \left(1 + \frac{s}{20} \right). \quad (80)$$

The minimum ∞ -norm now is 1.1203, while the compensator transfer function takes the form

$$C(s) = \frac{0.5177(s + 2.1277)((s + 0.4262)^2 + 0.4065^2)}{s((s + 28.4134)^2 + (24.5736^2)(s + 1.0204))}. \quad (81)$$

C is strictly proper. The closed-loop pole at -45.2010 is replaced with a pole pair at $-27.0438 \pm j22.9860$, while the remaining closed-loop poles alter not at all or very little. Figure 17 shows plots of the magnitudes of the system functions. Compared with Fig. 16 there is little change in S but U has the desired roll-off.

The results show that the control system specifications may be met with comfortable margins. They may be tightened by including extra specifications, such as

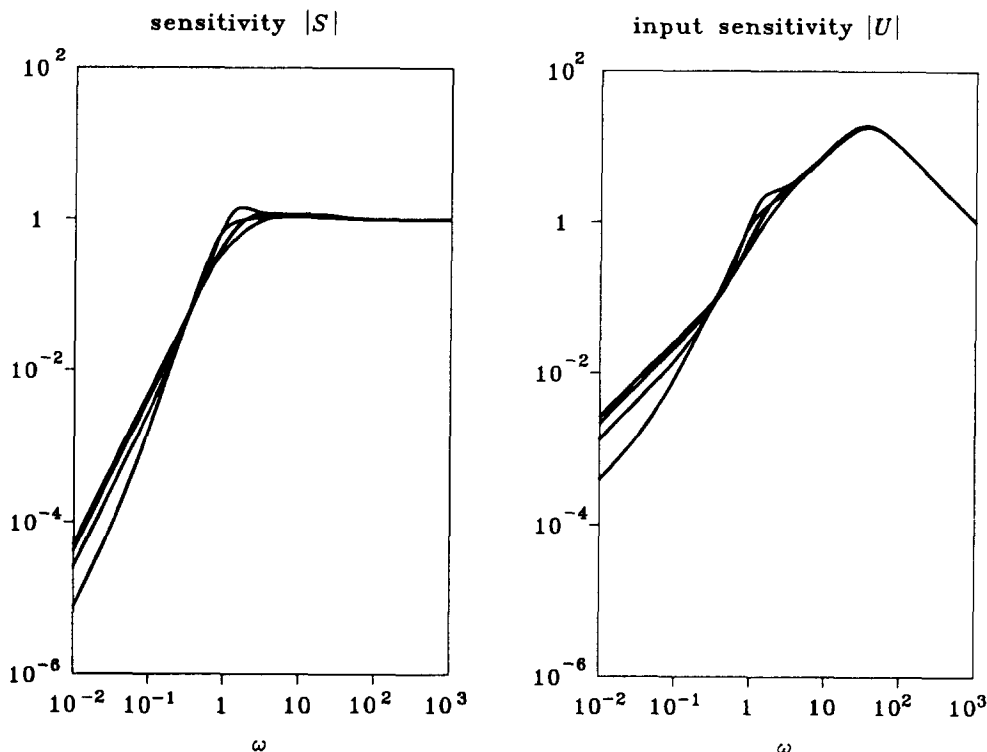


FIG. 17. Magnitudes of the sensitivity and input sensitivity for the second ship controller design.

minimal bandwidth. Lundh (1991) considers additional specifications on the peak values of S and U , on the response to input load disturbances, and on measurement noise sensitivity.

The optimal compensators in this section were again computed using the package based on the polynomial method (Kwakernaak, 1990b), with a small modification needed for the pole at 0 of the weighting function W_1 .

9. THE STANDARD \mathcal{H}_∞ -OPTIMAL REGULATOR PROBLEM

The mixed sensitivity problem is a special case of the so-called standard \mathcal{H}_∞ -optimal regulator problem. We introduce the standard problem by considering the mixed sensitivity function in the configuration of Fig. 18. The diagram shows V as a shaping filter for the disturbance, and W_1 and W_2 as frequency dependent weighting functions for the control system output and the plant input, respectively. The signal w is an external input that drives the disturbance shaping filter V .

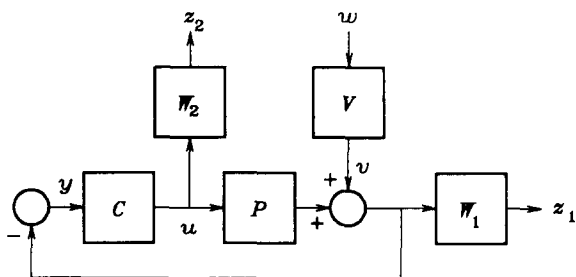


FIG. 18. The mixed sensitivity problem.

It is easy to check that the Laplace transforms of the weighted control system output z_1 and the weighted plant input z_2 are given by

$$\begin{aligned} \hat{z}_1 &= W_1 S V \hat{w}, \\ \hat{z}_2 &= -W_2 U V \hat{w}, \end{aligned} \tag{82}$$

so that $\hat{z} = \text{col}(\hat{z}_1, \hat{z}_2) = H \hat{w}$, with

$$H = \begin{bmatrix} W_1 S V \\ -W_2 U V \end{bmatrix}. \tag{83}$$

Hence, the mixed sensitivity problem amounts to the minimization of the ∞ -norm of the transfer matrix from the external input w to the composite output z . The freedom available in the minimization problem consists of the choice of the compensator C .

By isolating the compensator the block diagram of Fig. 18 may be represented as in Fig. 19, which is the configuration of the "standard" \mathcal{H}_∞ -optimal regulator problem. The signal w is an external input, representing driving signals for shaping filters for disturbances, measurement noise, and reference inputs. The signal z represents a control error. Ideally, z is identical to zero. The signal y represents the measured outputs that are available for feedback. The signal u , finally, represent the inputs that may be controlled.

The dynamics of the block G depends on the particular problem at hand. Inspection of Fig. 18 shows that for the mixed sensitivity problem

$$\begin{aligned} \hat{z}_1 &= W_1 V \hat{w} + W_1 P \hat{u}, \\ \hat{z}_2 &= W_2 \hat{u}, \\ \hat{y} &= -V \hat{w} - P \hat{u}. \end{aligned} \tag{84}$$

We rewrite this as

$$\hat{z} = \underbrace{\begin{bmatrix} W_1 V & W_1 P \\ 0 & W_2 \\ -V & -P \end{bmatrix}}_G \begin{bmatrix} \hat{w} \\ \hat{u} \end{bmatrix}, \quad (85)$$

which defines the transfer matrix G as

$$G = \begin{bmatrix} G_{11} & G_{12} \\ G_{21} & G_{22} \end{bmatrix} = \begin{bmatrix} W_1 V & W_1 P \\ 0 & W_2 \\ -V & -P \end{bmatrix}. \quad (86)$$

There are many other control problems that can be cast as special cases of the standard problem, including problems involving measurement noise and two-degree-of-freedom configurations. Of all these potential \mathcal{H}_∞ applications so far only the mixed sensitivity problem has been investigated in any depth.

The standard problem was first discussed by Francis and Doyle (1987) and is treated at length by Francis (1987).

10. FREQUENCY DOMAIN SOLUTION OF THE STANDARD PROBLEM

The bulk of the research on \mathcal{H}_∞ -optimization in the 1980s was devoted to the theoretical and mathematical aspects of the solution of the standard and other problems. Although the theory by no means has reached full maturity, algorithms and software are now becoming available for the solution of the standard problem. The software has not achieved a degree of user-friendliness, however, that affords the user to be totally unfamiliar with the details of the algorithms. For this reason we include in this paper a brief survey of two types of algorithms that are available. The present section is devoted to a frequency domain algorithm. The next section deals with state space algorithms.

Because \mathcal{H}_∞ -optimization problems are basically frequency domain oriented, it makes sense to consider frequency domain solutions. The simplest of these solutions relies on what is called J -spectral factorization, a notion that actually is basic for all solution methods. We outline this solution. It is based on Kwakernaak (1990a), which in turn is closely related to work by Green (1989).

It is not difficult to find that the closed-loop transfer matrix H of the configuration of Fig. 19, that is, the

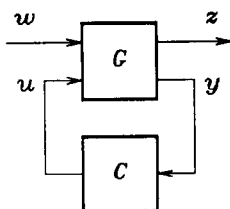


FIG. 19. The standard \mathcal{H}_∞ problem.

transfer matrix from w to z , may be expressed as

$$H = G_{11} + G_{12}(I - KG_{22})^{-1}KG_{21}. \quad (87)$$

It is characteristic for all approaches to the solution of \mathcal{H}_∞ -optimization problems that the problem of minimizing $\|H\|_\infty$ is not tackled directly, but that first the question is studied how to determine suboptimal compensators. Suboptimal compensators are compensators that stabilize the closed-loop system and achieve

$$\|H\|_\infty \leq \lambda, \quad (88)$$

with λ a given nonnegative number. Optimal compensators follow by finding the smallest value of λ for which such compensators exist.

The inequality $\|H\|_\infty \leq \lambda$ is readily seen to be equivalent to

$$H^T(-j\omega)H(j\omega) \leq \lambda^2 I, \quad \text{for all } \omega \in \mathbb{R}, \quad (89)$$

where the inequality is taken in the sense of definiteness of matrices. We write (89) more compactly as

$$H^-H \leq \lambda^2 I, \quad \text{on the imaginary axis,} \quad (90)$$

where if H is a matrix of rational functions H^- is defined by $H^-(s) = H^T(-s)$.

For reasons of exposition, consider the special case where $H = P - K$, with P the transfer matrix of a given unstable plant, and K a stable transfer matrix to be determined. It is easily recognized that this is a standard problem with $G_{11} = P$, $G_{12} = -I$, $G_{21} = I$, and $G_{22} = 0$. This problem, which is of more mathematical than practical interest, is known as the Nehari problem (Francis, 1987). Substituting $H = P - K$ into (90), we obtain $P^-P - P^-K - K^-P + K^-K \leq \lambda^2 I$ on the imaginary axis. This in turn we may rewrite as

$$[I \ K^-] \underbrace{\begin{bmatrix} \lambda^2 I - P^-P & P^- \\ P & -I \end{bmatrix}}_{\Pi_\lambda} \begin{bmatrix} I \\ K \end{bmatrix} \geq 0, \quad (91)$$

on the imaginary axis, which defines the rational matrix Π_λ . We now represent the compensator transfer matrix K in the form

$$K = YX^{-1}, \quad (92)$$

where Y and X are matrices of stable rational functions. By multiplying (91) on the right by X and on the left by X^- it follows that the inequality $\|H\|_\infty \leq \lambda$ is equivalent to the inequality

$$[X^- \ Y^-] \Pi_\lambda \begin{bmatrix} X \\ Y \end{bmatrix} \geq 0, \quad \text{on the imaginary axis.} \quad (93)$$

This simple derivation applies to the Nehari problem. It may be proved that also for the general case the inequality $\|H\|_\infty \leq \lambda$ is equivalent to (93), with the matrix Π_λ defined as

$$\begin{aligned} \Pi_\lambda = & \begin{bmatrix} 0 & I \\ -G_{12}^- & -G_{22}^- \end{bmatrix} \begin{bmatrix} \lambda^2 I - G_{11}G_{11}^- & -G_{11}G_{21}^- \\ -G_{21}G_{11}^- & -G_{21}G_{21}^- \end{bmatrix}^{-1} \\ & \times \begin{bmatrix} 0 & -G_{12} \\ I & -G_{22} \end{bmatrix}. \end{aligned} \quad (94)$$

The matrix Π_λ is para-Hermitian, that is, $\Pi_\lambda^- = \Pi_\lambda$. If

$\det \Pi_\lambda$ has no poles and zeros on the imaginary axis, Π_λ may be J -spectrally factored as

$$\Pi_\lambda = Z_\lambda^{-1} J Z_\lambda. \quad (95)$$

Z_λ is a square rational matrix such that both Z_λ and Z_λ^{-1} have all their poles in the open left-half plane. J is a constant matrix of the form

$$J = \begin{bmatrix} I & 0 \\ 0 & -I \end{bmatrix}, \quad (96)$$

with the two I blocks unit matrices of suitable dimensions. J is called the signature matrix of Π_λ .

Given the factorization (95), the condition (93) may be rewritten as

$$\begin{bmatrix} X^- & Y^- \end{bmatrix} Z_\lambda^{-1} J Z_\lambda \begin{bmatrix} X \\ Y \end{bmatrix} \geq 0, \quad \text{on the imaginary axis.} \quad (97)$$

Defining the square stable rational matrix A and the stable rational matrix B by

$$\begin{bmatrix} A \\ B \end{bmatrix} = Z_\lambda \begin{bmatrix} X \\ Y \end{bmatrix}, \quad (98)$$

it follows that (93) is equivalent to

$$A^- A \geq B^- B \quad \text{on the imaginary axis.} \quad (99)$$

By inverting Z_λ we find from (98) that

$$\begin{bmatrix} X \\ Y \end{bmatrix} = Z_\lambda^{-1} \begin{bmatrix} A \\ B \end{bmatrix}. \quad (100)$$

This expression, together with (99), provides an explicit formula for all compensators $K = YX^{-1}$ that make $\|H\|_\lambda \leq \lambda$.

There are many matrices of stable rational functions A and B that satisfy (99). An obvious choice is $A = I$, $B = 0$. This is known as the central solution†.

The question that remains is whether the compensators (100) actually stabilize the closed-loop system. It may be found that a necessary condition for a compensator given by (99)–(100) to stabilize the closed-loop system is that the numerator of $\det A$ have all its roots in the open left-half plane. It may furthermore be proved that if any stabilizing compensator exists that achieves $\|H\|_\infty < \lambda$, all compensators such that $\|H\|_\infty \leq \lambda$ follow from (99)–(100) with A such that $\det A$ has all its roots in the open left-half plane.

These results suggest the following search procedure:

- (1) Choose a value of λ .
- (2) Determine the J -spectral factor Z_λ and compute a corresponding compensator from (99)–(100) such that $\det A$ has all its zeros in the left-half plane. An obvious possibility is to compute the central solution.
- (3) Check if the compensator stabilizes the closed-loop system. If it does, decrease λ . If it does not, increase λ .

- (4) If the optimal solution has been approached sufficiently closely, stop. Else, return to (2).

The rational J -spectral factorization (95) may be reduced to two J -spectral factorizations of polynomial matrices: one for the denominator, one for the numerator. Algorithms for this factorization are now becoming available (Kwakernaak, 1990b; Šebek, 1990; Šebek and Kwakernaak, 1991, 1992).

The search process may terminate in two ways (Kwakernaak, 1990a; Glover *et al.*, 1991). The less common situation is that λ may be decreased steadily until it reaches a lower bound below which the desired J -spectral factorization is no longer possible. All suboptimal compensators for this least possible value of λ then are optimal.

The more usual situation is that λ may be decreased until it reaches a value where the factorization exists but no suboptimal solution stabilizes the closed-loop system. The search procedure may then be used to delimit the optimum. It turns out that as the optimum is approached, the J -spectral factorization becomes singular in the sense that the coefficients of the rational functions occurring in the spectral factor Z_λ grow without bound. At the same time, one of the closed-loop poles of the central solution approaches the boundary of the left-half plane, and actually crosses over from the left-half to the right-half plane, or vice-versa, at the optimal value λ_{opt} . Since the closed-loop transfer matrix H cannot have this closed-loop pole as a pole (because otherwise it would make $\|H\|_\infty$ infinite), this closed-loop pole cancels in H . It turns out that it actually cancels within the compensator transfer matrix C , and hence may be removed.

The singularity phenomenon in the J -spectral factorization may be avoided by only performing a partial factorization, which then may be exploited to compute exactly optimal solutions. The details are described elsewhere (Kwakernaak, 1990a), where also a characterization is given of all optimal solutions, similar to the characterization (100) of all suboptimal solutions. An experimental MATLAB macro package is available for the numerical computation of the optimal solutions (Kwakernaak, 1990b).

There are a large number of details that are not discussed here for lack of space. They concern assumptions on the dimensions of the signals w , u , z , and y , and on the transfer matrix G . Many of these assumptions may be removed or circumvented.

The singularity and cancelation phenomenon does not always occur. If it does not, optimal solutions are obtained corresponding to the largest value of λ such that $\det \Pi_\lambda$ has a pole or zero on the imaginary axis.

The suboptimal and optimal solutions normally are by no means unique. An exception is the SISO mixed sensitivity problem (Kwakernaak, 1990a).

11. STATE SPACE SOLUTION OF THE STANDARD PROBLEM

The mainstream work on algorithms for the solution of the standard problem focuses on state space algorithms (Doyle *et al.*, 1989; Glover and Doyle,

† Note that the central solution as defined here is not unique, because the spectral factorization (95) is not unique.

1989). We limit our exposition (which follows that of Weiland, 1990) to a special situation, whose solution admits a neat and compact presentation. The starting point is the description of the system

$$\begin{bmatrix} \dot{\hat{z}} \\ \hat{y} \end{bmatrix} = G \begin{bmatrix} \hat{w} \\ \hat{u} \end{bmatrix}, \quad (101)$$

in state form as

$$\begin{aligned} \dot{x} &= Ax + Bu + Ew_1, \\ z &= \begin{bmatrix} Dx \\ u \end{bmatrix}, \\ y &= Cx + w_2, \end{aligned} \quad (102)$$

with A , B , C , D , and E constant matrices. This state space representation is not completely general. Note the special structure of the control error z and the fact that the external signal w splits into two separate components $w = \text{col}(w_1, w_2)$. For a more general formulation see Glover and Doyle (1989). Note that even in these more general representations the transfer matrix G is limited to be proper, a restriction that is not necessary in the frequency domain solution.

First consider suboptimal \mathcal{H}_∞ regulation using state feedback, that is, when $y = x$. It turns out that in this case $\|H\|_\infty < \lambda$, if at all possible, may be achieved by static linear state feedback of the form

$$u = -Fx, \quad (103)$$

with F a constant matrix. The gain matrix F is given by

$$F = B^T X, \quad (104)$$

where the symmetric matrix X is a nonnegative-definite solution of the algebraic matrix Riccati equation

$$A^T X + XA + D^T D - X \left(BB^T - \frac{1}{\lambda^2} EE^T \right) X = 0, \quad (105)$$

such that the matrix $A - (BB^T - (1/\lambda^2)EE^T)X$ has all its eigenvalues in the open left-half plane. If no such solution X exists, there is no stabilizing state feedback such that $\|H\|_\infty < \lambda$.

One way of proving this result is to note that with u given by (103) the closed-loop transfer matrix from w to z is

$$H(s) = \begin{bmatrix} D(sI - A + BF)^{-1} E \\ -F(sI - A + BF)^{-1} E \end{bmatrix}. \quad (106)$$

Manipulation of the Riccati equation (105) in a way similar to the proof of the well-known Kalman-Yacubovitch equality (Kalman, 1964) results in the expression

$$\begin{aligned} \left[\lambda I - \frac{1}{\lambda} E^T (-sI - \bar{A}^T)^{-1} X E \right] \left[\lambda I - \frac{1}{\lambda} E^T X (sI - \bar{A})^{-1} E \right] \\ = \lambda^2 I - H^T(-s)H(s), \end{aligned} \quad (107)$$

where $\bar{A} = A - BF$. If $A - (BB^T - (1/\lambda^2)EE^T)X$ has all its eigenvalues in the open left-half plane, the left-hand side of (107) is positive-definite on the imaginary axis, which proves that $\|H\|_\infty < \lambda$.

Thus, in the case of full state information one algebraic Riccati equation needs to be solved, and static state feedback solves the problem. The output feedback problem, with measurement

$$y = Cx + w_2, \quad (108)$$

is more difficult to solve, although its solution is quite elegant and has a separation structure reminiscent of the LQG problem. It turns out that for output feedback the suboptimal solution needs to be modified to the feedback law

$$u = -F\hat{x}, \quad (109)$$

with $F = B^T X$ as before. The quantity \hat{x} may be viewed as the estimated state, and is the output of an observer-type system given by

$$\dot{\hat{x}} = \left(A - \frac{1}{\lambda^2} EE^T \right) \hat{x} + Bu + ZYC^T(y - C\hat{x}). \quad (110)$$

The symmetric matrix Y , if any exists, is a nonnegative-definite solution of the algebraic Riccati equation

$$AY + YA^T + E^T E - Y \left(C^T C - \frac{1}{\lambda^2} D^T D \right) = 0, \quad (111)$$

such that the matrix $A - Y(C^T C - (1/\lambda^2)D^T D)$ has all its eigenvalues in the open left-half plane. The constant matrix Z in (110) is given by

$$Z = \left(I - \frac{1}{\lambda^2} YX \right)^{-1}. \quad (112)$$

The compensator defined by (109)–(110) is suboptimal and stabilizes the feedback system if and only if $\|XY\|_\infty < \lambda$.

The order of the (suboptimal) compensator equals that of the “plant” G . Representations of “all” suboptimal solutions are also available (Glover and Doyle, 1989). The Riccati equations (105) and (111) are the equivalents of the two polynomial J -spectral factorizations in the frequency domain solution. The Riccati equations are normally solved by spectral decomposition of the corresponding Hamiltonian matrix. Numerically reliable routines are available in MATLAB.

An implementation of a search procedure to delimit the optimal solution analogous to that for the frequency domain approach is available commercially as part of the MATLAB Robust Control Toolbox (Chiang and Safonov, 1988), and the more recent MATLAB μ -Analysis and Synthesis Toolbox. As for the polynomial package, considerable expertise is needed for the use of these toolboxes. As the optimum is approached singularities occur that are similar to those for the frequency domain solution. Glover *et al.* (1991) have analysed these phenomena.

The state space solution of the \mathcal{H}_∞ problem requires more assumptions (for instance that the transfer matrix G be proper) than the frequency domain solution. On the other hand, the numerical algorithms for solving Riccati equations are better developed than the J -spectral factorization algorithms needed in the frequency domain approach.

12. CONCLUSIONS

\mathcal{H}_∞ -optimal regulation is a rewarding research subject both for theoreticians and engineers. Theoreticians and also mathematicians find an unequalled opportunity to penetrate deeper into the rich and intricately structured world of linear systems. Engineers recognize many of the issues and design targets of "classical" control theory, which now can be handled algorithmically.

Although the subject has received much attention it has not reached maturity. There are several important topics that we have not been able to touch upon in this tutorial exposition, and are subjects of intensive research.

On the theoretical side, the discrete-time \mathcal{H}_∞ -optimal regulation problem is more or less understood. Francis (1990) is doing interesting work on the application of \mathcal{H}_∞ -theory to sampled-data systems. Theoretical work on distributed-parameter system is in progress (Curtain, 1991), and attempts are being made to deal with nonlinear problems (Van der Schaft, 1990).

Further theoretical work on finite-dimensional linear systems is directed towards exploring the connections between various solution methods such as those based on the state space approach, J -spectral factorization, operator theoretic methods, interpolation theory, and differential game theory. It cannot be claimed that all aspects of optimal solutions (as opposed to suboptimal solutions) are fully understood, and no doubt considerable attention remains to be spent on this topic.

A problem of considerable interest, where relatively little progress has been made, is how to use the freedom still present in \mathcal{H}_∞ -optimal solutions resulting from the lack of uniqueness. The reason for this lack of uniqueness is that the ∞ -norm involves the peak value of the largest singular value of the closed-loop frequency response matrix only. This leaves considerable freedom in the behavior of the smaller singular values. The control theoretical interpretation of this freedom is not clear. One way of eliminating the nonuniqueness is to look for solutions among all \mathcal{H}_∞ -optimal solutions that successively minimize the peak values of all lesser singular values. This leads to the notion of superoptimality (see e.g. Kwakernaak, 1986; Jaimoukha and Limebeer, 1991).

Another way of eliminating nonuniqueness is to choose so-called "minimum-entropy" solutions (Mustafa and Glover, 1990). Other researchers use the remaining freedom for further optimization purposes.

Another line of research is directed towards making the theory applicable. As we have shown, the SISO mixed sensitivity problem has considerable design potential. The multivariable mixed sensitivity problem shares this, but not all the conclusions for the SISO case generalize straightforwardly. Other special cases of the standard problem, such as criteria involving all three of the sensitivity function, the complementary sensitivity function, and the input sensitivity function, are being looked into. A monograph has been devoted to a special version of the mixed sensitivity problem deriving from what is known as normalized

coprime factor plant descriptions (McFarlane and Glover, 1990).

A further question that by no means has been settled is how to translate practical information about plant uncertainty and modeling inaccuracy into quantitative terms that allow the application of \mathcal{H}_∞ techniques. Doyle's "structured singular value" (Doyle, 1982) no doubt is an important step in the right direction.

The fact that algorithms and software become slowly available strongly stimulates work on "real world" applications. More and more interesting design studies are reported, with encouraging results. Several papers presented at a recent meeting in Cambridge attest to this (see for instance Kellett, 1991; Marshfield, 1991; Walker and Postlethwaite, 1991). Other applications are reviewed by Postlethwaite (1991).

The wealth of results on \mathcal{H}_∞ -optimization is finding its way into books. Besides the monographs by Mustafa and Glover (1990) and McFarlane and Glover (1990) a book by Morari and Zafiriou (1989) is attracting considerable attention. A recent text by Doyle *et al.* (1991) introduces some of the \mathcal{H}_∞ material at the level of a second course on control.

REFERENCES

- Åström, K. J. (1990). Regulation of a ship's heading. In E. J. Davison (Ed.), *Benchmark Problems for Control System Design*. Theory Committee, IFAC.
- Chiang, R. Y. and M. G. Safonov (1988). *Robust-Control Toolbox User's Guide*. The Math Works, South Natick, MA.
- Curtain, R. F. (1991). State space approaches to \mathcal{H}_∞ -control for infinite-dimensional linear systems. *Proc. Conf. Robust Control System Design Using \mathcal{H}_∞ and Related Methods*, 21–22 March, Cambridge, U.K.
- Desoer, C. A. and M. Vidyasagar (1975). *Feedback Systems: Input-Output Properties*. Academic Press, New York.
- Doyle, J. C. (1979). Robustness of multiloop linear feedback systems. *Proc. 17th IEEE Conf. Decision and Control*, pp. 12–18.
- Doyle, J. C. (1982). Analysis of feedback systems with structured uncertainties. *IEE Proc.*, **129**, 242–250.
- Doyle, J. C. (1984). *Lecture Notes*, ONR/Honeywell workshop on advances on multivariable control, Minneapolis, MN.
- Doyle, J. C., B. A. Francis and A. Tannenbaum (1991). *Feedback Control Theory*. Macmillan, New York.
- Doyle, J. C., K. Glover, P. P. Khargonekar and B. A. Francis (1989). State space solutions to standard \mathcal{H}_2 and \mathcal{H}_∞ control problems. *IEEE Trans. Aut. Control*, **34**, 831–847.
- Engell, S. (1988). *Optimale Lineare Regelung*. Fachberichte Messen, Steuern, Regeln, **18**. Springer-Verlag, Berlin.
- Francis, B. A. (1987). A course in H_∞ control theory. *Lecture Notes in Control and Information Sciences*, **88**. Springer-Verlag, Berlin.
- Francis, B. A. (1990). Lectures on H_∞ -control and sampled data systems. In E. Mosca and L. Pandolfi (Eds), *H_∞ -Control Theory, Como 1990; Lecture Notes in Mathematics*, **1496**. Springer-Verlag, Berlin.
- Francis, B. A. and J. C. Doyle (1987). Linear control theory with an H_∞ optimality criterion. *SIAM J. Control Opt.*, **25**, 815–844.
- Freudenberg, J. S. and D. J. Looze (1988). Frequency domain properties of scalar and multivariable feedback systems. *Lecture Notes in Control and Information Sciences*, **104**. Springer-Verlag, Berlin.
- Glover, K. and J. C. Doyle (1989). A state space approach to H_∞ optimal control. In H. Nijmeijer and J. M.

- Schumacher (Eds), *Three Decades of Mathematical System Theory, Lecture Notes in Control and Information Sciences*, **135**. Springer-Verlag, Berlin.
- Glover, K., D. J. N. Limebeer, J. C. Doyle, E. M. Kasenally and M. G. Safonov (1991). A characterization of all solutions to the four block general distance problem. *SIAM J. Control and Optimization*, **29**, 283–324.
- Green, M. (1989). H_∞ controller synthesis by J -lossless coprime factorization. Department of Electrical Engineering, Imperial College, London. *SIAM J. Control and Optimization*, (to appear).
- Jaimoukha, I. M. and D. J. N. Limebeer (1991). State-space algorithm for the solution of the two-block super-optimal distance problem. *Preprints 30th IEEE Conference on Decision and Control*, Brighton, U.K.
- Kalman, R. E. (1964). When is a linear control system optimal? *J. Basic Eng. Trans. ASME, Ser. D*, **86**, 51–60.
- Kellett, M. G. (1991). Continuous scheduling of H^∞ controllers for a MS760 Paris aircraft. *Proc. Conf. Robust Control System Design Using \mathcal{H}_∞ and Related Methods*, 21–22 March, Cambridge, U.K.
- Kwakernaak, H. (1983). Robustness optimization of linear feedback systems. *Preprints 22nd IEEE Conference on Decision and Control*, San Antonio, TX.
- Kwakernaak, H. (1985). Minimax frequency domain performance and robustness optimization of linear feedback systems. *IEEE Trans. Aut. Control*, **AC-30**, 994–1004.
- Kwakernaak, H. (1986). A polynomial approach to minimax frequency domain optimization of multivariable systems. *Int. J. Control*, **44**, 117–156.
- Kwakernaak, H. (1990a). The polynomial approach to \mathcal{H}_∞ -optimal regulation. In E. Mosca and L. Pandolfi (Eds), H_∞ -Control, Como 1990; *Lecture Notes in Mathematics*, **1496**. Springer-Verlag, Heidelberg.
- Kwakernaak, H. (1990b). MATLAB macros for polynomial \mathcal{H}_∞ control system optimization. Memorandum No. 881, Department of Applied Mathematics, University of Twente, Enschede, The Netherlands.
- Lundh, M. (1991). Robust adaptive control. Doctoral dissertation, Department of Automatic Control, Lund Institute of Technology, Lund, Sweden.
- Marshfield, W. B. (1991). Submarine periscope depth keeping using an H -infinity controller together with sea noise reduction notch filters. *Proc. Conf. Robust Control System Design Using \mathcal{H}_∞ and Related Methods*, 21–22 March, Cambridge, U.K.
- McFarlane, D. C. and K. Glover (1990). Robust controller design using normalized coprime factor plant descriptions, *Lecture Notes on Control and Information Sciences*, **138**. Springer-Verlag, Berlin.
- Morari, M. and E. Zafriou (1989). *Robust Process Control*. Prentice Hall, Englewood Cliffs, NJ.
- Mustafa, D. and K. Glover (1990). Minimum entropy \mathcal{H}_∞ control, *Lecture Notes in Control and Information Sciences*, **146**. Springer-Verlag, Berlin.
- Postlethwaite, I. (1991). Robust control of multivariable systems using \mathcal{H}^∞ optimization. *J.A.*, **32**, 8–19.
- Postlethwaite, I., M.-C. Tsai and D.-W. Gu (1990). Weighting function selection in H^∞ design. *Preprints, 11th IFAC World Congress*, Tallinn, Vol. **5**, pp. 104–109.
- Šebek, M. (1990). An algorithm for spectral factorization of polynomial matrices with any signature. Memorandum No. 912, Department of Applied Mathematics, University of Twente, Enschede, The Netherlands.
- Šebek, M. and H. Kwakernaak (1991). J -spectral factorization. *Preprints, 30th IEEE Conf. on Decision and Control*, Brighton, 11–13 December, pp. 1278–1283.
- Šebek, M. and H. Kwakernaak (1992). Further numerical methods for J -spectral factorization. *Preprints, Second IFAC Workshop on System Identification and Control*, Prague.
- Sefton, J. and K. Glover (1990). Pole/zero cancellations in the general \mathcal{H}_∞ problem with reference to a two block design. *Systems and Control Letters*, **14**, 295–306.
- Van der Schaft, A. J. (1992). L_2 -Gain analysis of nonlinear systems and nonlinear state feedback H_∞ control. *IEEE Trans. Aut. Control*, **37**, 770–784.
- Verma, M. and E. Jonckheere (1984). L_∞ -compensation with mixed sensitivity as a broadband matching problem. *Systems and Control Letters*, **4**, 125–130.
- Vidyasagar, M. (1985). *Control Systems Synthesis—A Factorization Approach*. MIT Press, Cambridge, MA.
- Vidyasagar, M., H. Schneider and B. A. Francis (1982). Algebraic and topological aspects of feedback stabilization. *IEEE Trans. Aut. Control*, **AC-27**, 880–894.
- Walker, D. and I. Postlethwaite (1991). Discrete time H^∞ control laws for a high performance helicopter. *Proc. Conf. Robust Control System Design Using \mathcal{H}_∞ and Related Methods*, 21–22 March, Cambridge, U.K.
- Weiland, S. (1990). State space \mathcal{H}_∞ control theory. Minicourse on robust control and state space \mathcal{H}_∞ -control theory, 1990 Benelux Meeting on Systems and Control, Veldhoven, The Netherlands.
- Zames, G. (1979). Feedback and optimal sensitivity: Model reference transformations, weighted seminorms, and approximate inverses. *Proc. 17th Allerton Conf.*, pp. 744–752.
- Zames, G. (1981). Feedback and optimal sensitivity: Model reference transformations, multiplicative seminorms, and approximate inverses. *IEEE Trans. Aut. Control*, **AC-26**, 301–320.